A High-Frequency Resonant Converter Based on the Class Φ_2 Inverter for Wireless Power Transfer

Jungwon Choi, Wei Liang, Luke Raymond, Juan Rivas
Department of Electrical Engineering
Stanford University
Stanford, California, 94305
Email: jwonchoi@stanford.edu

***Abstract*—This paper presents the design and implementation of a high frequency resonant converter based on the Class Φ_2 inverter for inductive power transfer. MHz frequency operation can allow for higher power density than conventional switching frequencies. The converter is based on the Class Φ_2 inverter, reducing the voltage stress across the switch compared to other resonant topologies. In order to increase power while reducing input current ripple, a push-pull Class Φ_2 inverter was implemented to drive resonant coils for wireless power transfer (WPT). Specially, we demonstrated 219 W, 160 V push-pull inverter at 13.56 MHz. This paper provides experimental and simulated results of the WPT system investigated.**

I. Introduction

Wireless power transfer (WPT) has attracted recent attention as a power deliver method for numerous mobile, medical applications, and electric vehicle charging systems [1]–[3]. More specifically, WPT through inductive resonant coupling has been analyzed and demonstrated as a method of delivering power to a load with relatively high efficiency [4], [5]. Various frequency ranges can be used for WPT. However, this paper implements a 13.56 MHz frequency WPT system in order to study the trade-offs in design, size and feasibility of WPT at high frequencies. Operating at frequencies above 10 MHz allows for a significant reduction in the values of passive energy storage components [6]. This reduction allows for all magnetic components in our design to be implemented without using ferro-magnetic cores.

The WPT system presented herein consists of class Φ_2 power amplifier driving a tuned set of transmitting and receiving coils. We use resonant power amplifier because it enables operation at switching frequencies above 10 Mhz. Moreover, a Φ_2 inverter allows for a higher input voltages for a given switch rating. The Φ_2 inverter operates at reduced device voltage stresses compared to other commonly used single-switch high frequency resonant topologies.

The design presented herein is a push-pull version of the Φ_2 inverter [7] which allows for an increase in the output power delivered to the load while exhibiting other promising attributes such as lower input current ripple. Each side of the push-pull inverter operates from a single input voltage source and shares a common ground, which reduces the complexity of the gate drive. A push-pull implementation can potentially lead to consolidation of passive components which promises increased power density over a single inverter design.

In this paper, a push-pull class Φ_2 inverter for inductive wireless power transfer at 13.56 MHz is designed and evaluated. Section II provides details regarding the configuration of a single inverter, the transmitter and receiver coils, and push-pull version of the inverter. Section III presents details regarding the simulation and experimental results of a single inverter and the push-pull inverter with coils. Section IV concludes the paper.

II. Circuit Configuration

A. Class Φ_2 inverter

The Class E inverter [8] of Fig. 1 is a well known resonant topology capable of operating at frequencies reaching into the 10s of MHz. This topology provides zero voltage switching (ZVS) and has a single ground-referenced active switch (Q_1). While the class E topology has many merits as an rf inverter, it achieves ZVS but imposes a large voltage stress across the active switch. The peak switch voltage can reach in excess of 3.6 times the input voltage. Moreover, this circuit is normally designed with a relatively large input inductance (L_{choke} in Figure 1), but designs with smaller inductance values are possible [9]. This input "choke" tends to slow the transient response of the system.

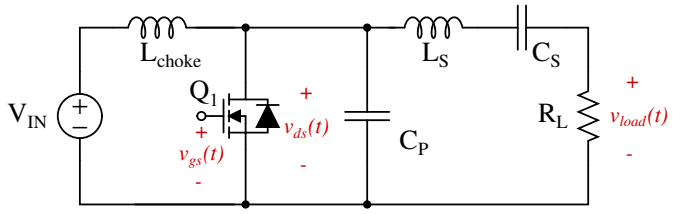

Fig. 1: Class E inverter. Peak drain voltage reaches $\geq 3.6 \times V_{IN}$. This topology is widely used in rf and high frequency applications.

A topology that overcomes many of the shortfalls of the class E is the class Φ_2 inverter of [10]. This circuit topology is shown in Fig. 2. It has an additional circuit branch formed by L_{MR} and C_{MR} in parallel with the active switch. These components are tuned to provide a low impedance at the 2^{nd} of the switching frequency. Following the procedure outlined in [10], the drain impedance under biased conditions is tuned to produce a waveform with a substantial reduction in peak voltages compared with the class E of Fig. 1. The resulting trapezoidal voltage waveform at the drain has a peak of approximately twice the input voltage. This allows the use

of a MOSFET with lower voltage rating and hence better conduction, and switching characteristics for a given input voltage. Moreover, as described in [10], the interaction of L_F and C_P with the remaining resonant components of the circuit and the load make the impedance at fundamental and third harmonics to attain the values that make the MOSFET voltage approximate a trapezoid. It is important to notice that in the Φ_2 of Fig. 2, the inductance L_F place an active role in shaping the drain voltage, and has a significantly smaller value than in most class E designs. Smaller input inductance value results in a faster transient response but at the expense of a significantly larger input current ripple. Evidently, the larger input current ripple of a Φ_2 design is not an issue when two converters are operated in push-pull due to the current interleaving effect.

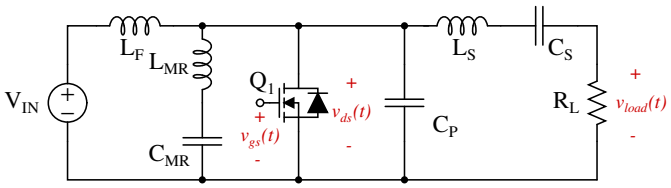

Fig. 2: Class Φ_2 inverter. Peak drain voltage is reduced to $\sim 2 \times V_{in}$

B. Resonant coupling

Figure 3 shows the model of the coupled coils connected to the capacitors used to resonate the magnetizing and leakage inductance of the structure. Specifically, in this figure L_M represents the magnetizing inductance of the cantilever model [11], while L_l is the leakage. Here, n models the the effective turn ratio. We used the cantilever transformer model throughout our design because it allows us to easily incorporate part or the totality of the leakage and magnetizing inductance into the design of the Φ_2 inverter. In this model, when the distance and/or position between the transmitter and receiver coils varies, L_l and n change simultaneously, and this change can be substantial. The variation in the parameter of the model depends, among other things, on the number of turns of each coil, its diameter etc. Moreover, due to the limited number of low-loss magnetic materials able to operate in this frequency range, our design does not use sheets of magnetic material behind the transmitter and receiver coils used to steer the magnetic flux and improve coupling.

If the number of turns on the primary coil is less than the secondary coil, the effective ratio increases with distance. This effective ratio is a significant factor when designing the inverter. Therefore, if the distance changes significantly, the inverter performance is adversely affected. In highly resonant converters active re-tuning may be difficult or impractical. Frequency variation can help mitigate de-tuning due to coil parameter variation, but the benefits of this approach is limited as the frequency range in which the Class Φ_2 inverter operates efficiently is narrow.

C. Push-pull inverter with resonant coil

In this paper a push-pull class Φ_2 inverter was designed to deliver 175 W to a 50 Ω load, when $V_{IN} = 180$V. Figure 5 shows a schematic of the Φ_2 push-pull inverter formed by combining two single ended inverters [12]. This configuration leverages the tuning efforts of one converter, and applies it in a way that increases output power and power density with a

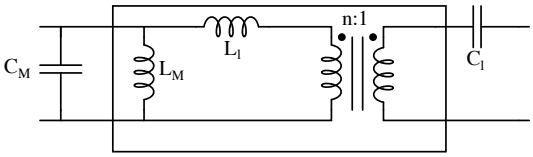

Fig. 3: Model of transmitting and receiving coil. L_M and L_R presents magnetizing inductance and leakage inductance. n is the the effective turns ratio between the two coils. L_l and n is changed according to the variation of distance between coils. C_M and C_l are selected to be resonant at 13.56 MHz.

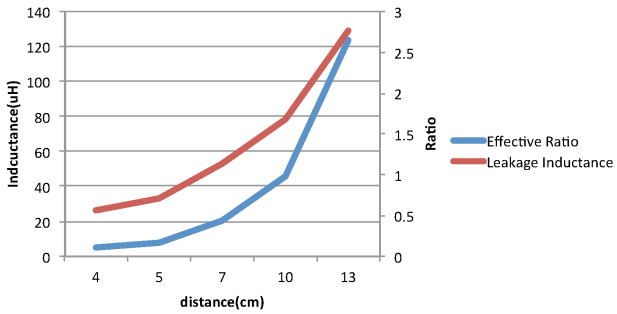

Fig. 4: Variation of leakage inductance L_M and effective ratio n with coil separation. In our coils, the self-inductance of transmitter coil is L_1=0.403 uH, while the self-inductance of receiver coil is L_2=16.3 μH. As coil separation increases, L_M increases rapidly. So does, n, the effective turns ration of the structure.

modest increase in complexity. Moreover, as described in [7] several components can be consolidated to improve power density. The gates for each MOSFET in the push-pull inverter are driven with out-of-phase signals to operate in alternation. In Fig. 6, coils are placed between the inverter and load to

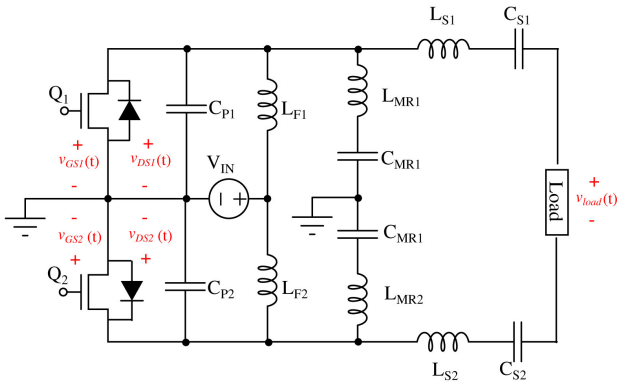

Fig. 5: Push-pull class Φ_2 inverter. A single inverter is tuned first for the load and another inverter is duplicated. MOSFET gate signals are phase shifted 180° to operate inverters alternatively.

form an air core transformer central to the WPT effort. The high Q resonance of the circuit containing the coils results in an ac output with low harmonic content.

III. Experimental Verification

The WPT system implemented here was designed to deliver 250 W of power through a 4 cm air-gap with a switching frequency of 13.56 MHz frequency. The design was simulated and implemented experimentally to verify the feasibility of this approach.

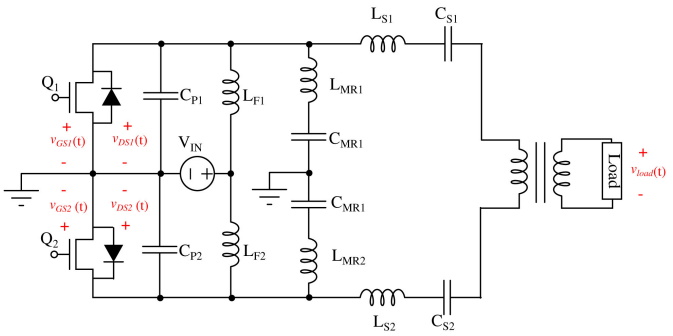

Fig. 6: Push-pull class Φ_2 with receiving and transmitting coil. The primary coil is connected to the output of the inverter. The load is attached to the secondary coil. The impedance seen by inverter should be resistive to transfer maximum power. The load coils form a transformer that also provides isolation between the inverter and load.

A. *Single ended Φ_2 Inverter*

We started by designing and simulating a single ended Φ_2 WPT circuit in LTspice. Our simulation incorporated relevant parasitic parameters extracted by measurement on the PCB used during the implementation. Moreover, our library models pay careful attention to model the non-linear C_{oss} and C_{gd} as function of the applied drain voltage.

Figure 7 shows the simulated $v_{ds}(t)$ and $v_{load}(t)$ of a single ended Φ_2 inverter of Fig. 2.

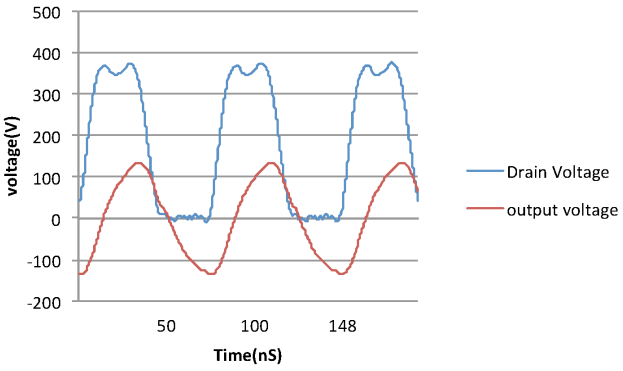

Fig. 7: Simulated drain voltage for a single inverter. Here $f_s = 13.56$ MHz, $V_{IN} = 180$ V and $R_L = 50\ \Omega$. Here L_F =390 nH, L_{MR} =300 nH, $C_{MR} = 114$ pF, L_S =900 nH and C_s =1 nF.

The simulation and implementation of the class Φ_2 inverter driving a 50 Ω resistive load was designed for use with a 500 V Microsemi ARF475FL. This MOSFET comes in a dual rf package with low package inductance. In the preliminary single ended implementation of the Φ_2 inverter only one side of ARF475FL was utilized. We proceeded to implement and test the complementary single ended inverter that would eventually form a push-pull. We made sure both single ended converters performed at comparable output power levels and present similar $v_{ds}(t)$ waveforms. Figure 8 shows the measured v_{ds} and $v_{\text{load}}(t)$ when $V_{IN} = 180$ V. In this operating condition, the maximum $v_{ds}(t)$ is ≈ 360 V. Notice the good agreement between experiment and simulation.

B. *WPT with single ended Φ_2 driving stage.*

Figure 9 shows the two coils used for the WPT described here. The 2 turn transmitter coil has a inductance of 748 nH

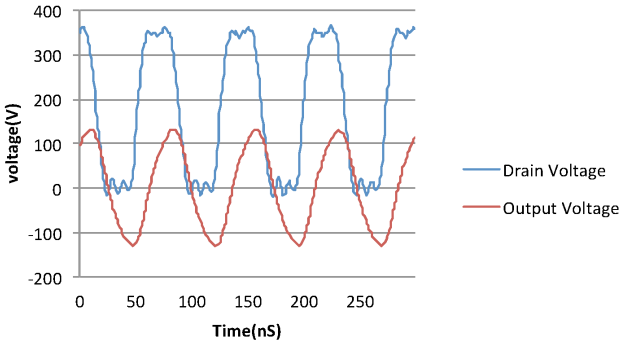

Fig. 8: Measured drain and output voltage of the inverter under WPT operation. Here $V_{in} = 180$ V and $R_L = 50\ \Omega$, L_{MR}=300 nH, L_F=390 nH, L_s=900 nH, C_{MR}=114 pF, C_p=185 pF, C_s=1 nF, L_1=748 nH, $L_2 = 3.1\ \mu$H, C_M=184 pF, C_l=44 pF.

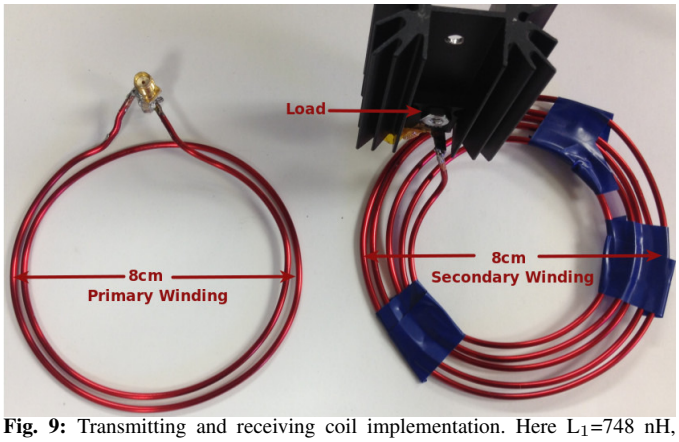

Fig. 9: Transmitting and receiving coil implementation. Here L_1=748 nH, L_2=3.1 μH, C_M =185 pF, C_l=44 pF and R=10 Ω.

while the 5 turn receiver has a self inductance of 3 μH. L_M, L_l and n, the parameters of the cantilever model are obtained from open and short impedance measurements as described in [11]. L_M is 0.748 μH and L_l is 14.75 μH. These values are used to determine the value of capacitances C_M and C_l that resonate L_M and L_S at the switching frequency. For these values, the inductances of the cantilever model resonate at $f_s = 13.56$ MHz with $C_M = 185$ pF and $C_l = 44$ pF connected to each coil as shown in Fig. 3. C_M was connected to the primary coil in parallel to resonate the The effective turn ratio of the coil arrangement is n =2.24 when the separation of the coils is 4 cm. A 10 Ω load resistor is connected to the receiver coil. This way, when properly tuned, the equivalent resistance at the fundamental seen at input of the transmitter coil is $\approx 50\ \Omega$.

The output power and efficiency as function of input voltage is depicted in Fig. 10. Increasing input voltage leads to higher power and efficiency. Also, the variation of power and efficiency with coil separation are plotted in Fig. 11.

The transmitter and receiver coils were tuned at a 4 cm distance. Therefore, this is the point in the figure of peak output power and efficiency.

C. *WPT with a Φ_2 Push-pull converter.*

Figure 12 shows the assembled PCB of the push-pull Φ_2 inverters described here. Table I list the values of the

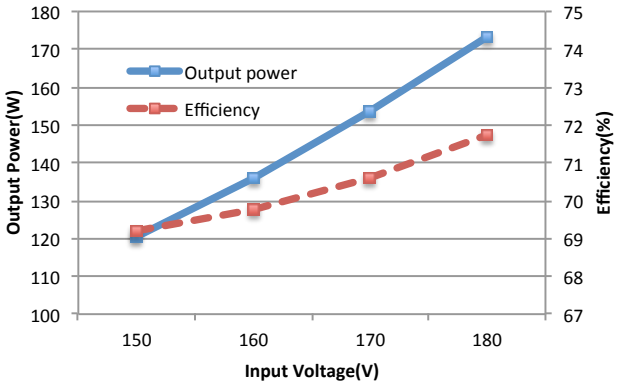

Fig. 10: Measured power and efficiency vs. V_{IN}. Airgap is 4 cm. Efficiency varies slightly between 68 % and 71 % in the 150 $V \leq V_{IN} \leq$ 180 V range.

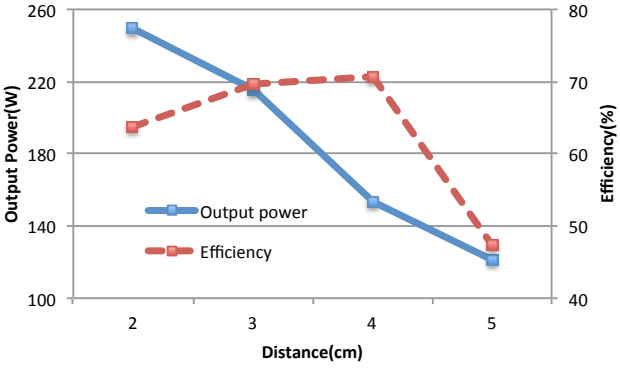

Fig. 11: Measured power and efficiency vs. distance. Here, $V_{in} = 170$ V, $f_s = 13.56$ MHz. As coil separation increases, power delivery decreases. Efficiency is maximum at 4 cm, the nominal coil separation.

components of the Φ_2 inverters that form our push-pull design.

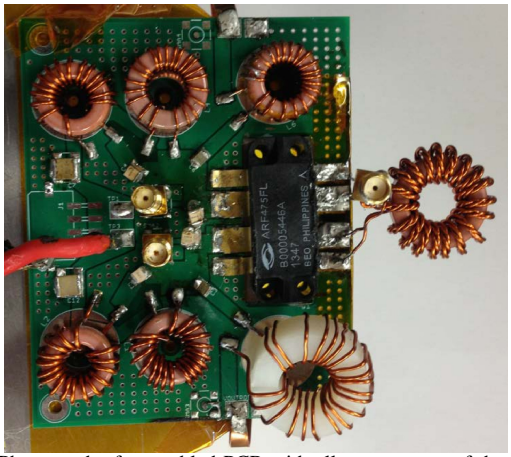

Fig. 12: Photograph of assembled PCB with all components of the Φ_2 push-pull inverter. Note the gate drive tri-filar transformer next to the MOSFET.

The PCB was laid out paying close attention to symmetry to ensure parasitics of the two single ended converters were the same. Out-phased gate signals, were obtained by using a tri-filar wound air-core transformer (shown on the right of Fig. 12). Applying the output of a rf power amplifier to one of the windings, we obtained two equal isolated gating signal, that can be connected to drive the gates of the two MOSFETs

TABLE I: Components values. Here L1 is the self inductance of the transmitter coil while L_2 is the self inductance of the receiver.

Parameter	Value	Units
L_f	390	nH
L_{MR}	300	nH
L_s	900	nH
C_{MR}	114	pF
C_p	185	pF
C_s	1	nF
L_1	748	nH
L_2	3.1	μH
C_M	184	pF
C_l	44	pF
MOSFET	ARF475FL	

with the appropriate phase difference. Figure 14 shows the experimental measurement of the two drain voltages. Notice that they have similar shape but are shifted by 180°. The single ended Φ_2 inverters were designed for a 50 Ω load. When connecting two out-of-phase inverters in a push-pull, the load can be connected differentially between the output rails of the inverters. To keep the respective drain impedance of each stage unchanged the load impedance of the push-pull configuration must double. Based on the effective turn ratio of our transmitting and receiving coils, a 20 Ω resistance connected to the receiving end will have an equivalent impedance of 100 Ω at the output of the push-pull. Figure 15 shows the output voltage waveform across the 20 Ω load of the push-pull when $V_{IN} = 160$ V. The output power under this operating condition was 219 W with an efficiency of 71 %. The output power was measured under varying voltage and distance as depicted in Fig. 16 and 17. For push-pull inverter, the coil was tuned for a separation of 2.5 cm.

Future work will include improvements in the layout and reduce the inductance between the outputs of the two single-ended stages and the transmitter coil. We also plan to study the effect of low-loss, low-permeability materials to steer the magnetic flux and improve coupling between the coils and increase their separation.

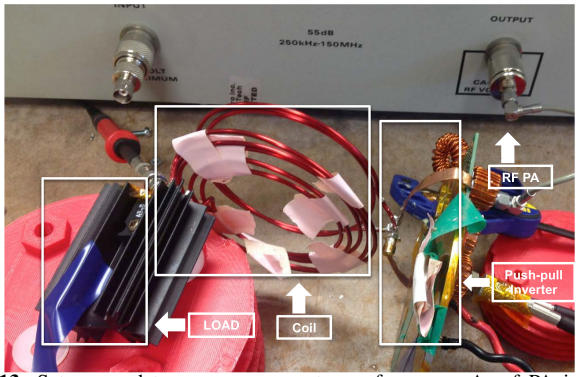

Fig. 13: Set up used to measure converter performance. An rf PA is used to provide power to the respective gates via the tri-filar transformer. During testing, the converter and coils were placed at enough distance from metallic structures that could affect coupling.

IV. Conclusion

This paper presents the design and implementation of a wireless power transfer system based on the class Φ_2 inverter. High frequency operation provides high power density by

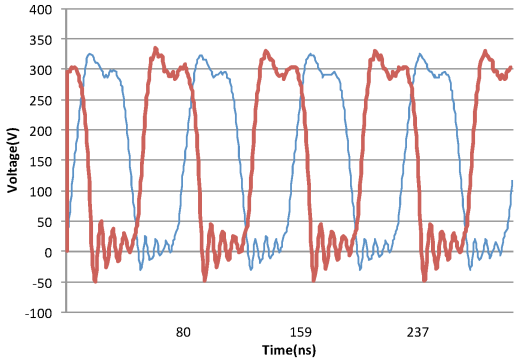

Fig. 14: Measured drain voltage of push-pull inverter under WPT operation. Here $V_{IN} = 160\ V$ and $R_L = 20\ \Omega$, $f_s = 13.56$ MHz, L_F=390 nH, L_{MR}=300 nH, L_s=900 nH, C_{MR}=114 pF, C_p=185 pF, C_s=1 nF, L_1=748 nH, $L_2 = 3.1\ \mu$H, C_M=184 pF, C_l=44 pF. The two drain voltage have same waveform.

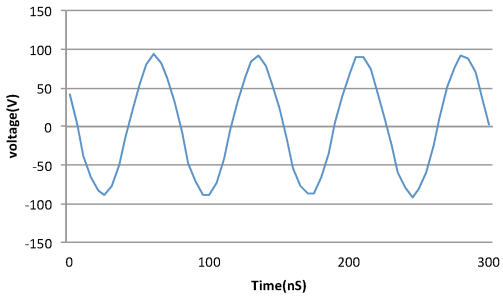

Fig. 15: Measured output voltage of push-pull inverter under WPT operation. Here $V_{IN} = 160\ V$ and $R_L = 20\ \Omega$, L_{MR}=300 nH, L_s=900 nH, C_{MR}=114 pF, C_p=185 pF, C_s=185 pF, L_1=748 nH, $L_2 = 3.1\ \mu$H, C_M=184 pF, C_L=44 pF. Power is 219 W with 71 % efficiency.

reducing passive component size. The power amplifier for WTP is implemented based on class Φ_2 inverter in order to achieve low voltage stress and fast transient response. To enhance the concept of class Φ_2 inverter, a push-pull inverter was designed to deliver more power to the load with little additional tuning effort. A 219 W 160 V Φ_2 push-pull inverter switching at 13.56 MHz was implemented and experimentally tested. The efficiency is about 71 %. Efficiency increases are expected through the development of different gating methods and improved coil modeling and design.

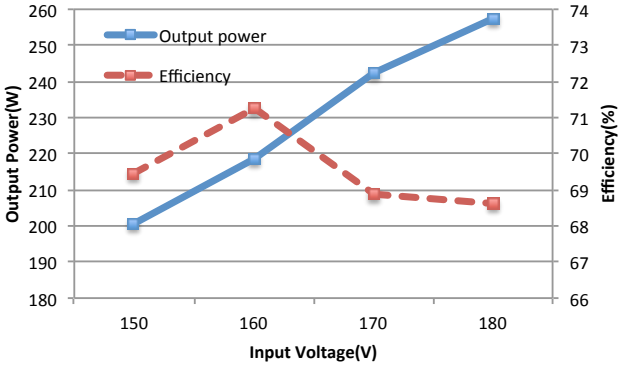

Fig. 16: Measured output voltage in the push-pull inverter. Here, coil separation is 2.5 cm. Power delivery increases with input voltage. The efficiency varies slightly within this input voltage range.

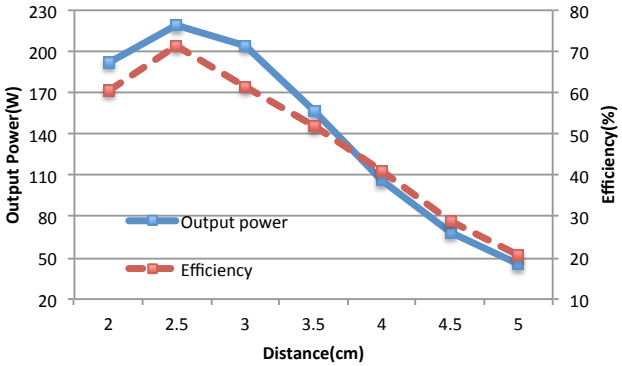

Fig. 17: Measured power and efficiency of the Φ_2 push-pull inverter vs. coil separation. Here $V_{in} = 160\ V$ and $R_L = 20\ \Omega$.

REFERENCES

[1] W. Chen, R. A. Chinga, S. Yoshida, J. Lin, C. Chen, and W. Lo, "A 25.6 w 13.56 mhz wireless power transfer system with a 94amplifier," in *Microwave Symposium Digest (MTT), 2012 IEEE MTT-S International*, June 2012, pp. 1–3.

[2] S. Kim, J. Ho, and A. Poon, "Wireless power transfer to miniature implants: Transmitter optimization," *Antennas and Propagation, IEEE Transactions on*, vol. 60, no. 10, pp. 4838–4845, Oct 2012.

[3] A. Sample, D. Meyer, and J. Smith, "Analysis, experimental results, and range adaptation of magnetically coupled resonators for wireless power transfer," *Industrial Electronics, IEEE Transactions on*, vol. 58, no. 2, pp. 544–554, Feb 2011.

[4] A. Kurs, A. Karalis, R. Moffatt, J. D. Joannopoulos, P. Fisher, and M. Soljai, "Wireless power transfer via strongly coupled magnetic resonances," *Science*, vol. 317, no. 5834, pp. 83–86, 2007. [Online]. Available: http://www.sciencemag.org/content/317/5834/83.abstract

[5] G. Covic and J. Boys, "Inductive power transfer," *Proceedings of the IEEE*, vol. 101, no. 6, pp. 1276–1289, June 2013.

[6] D. J. Perreault, J. Hu, J. M. Rivas, Y. Han, O. Leitermann, R. Pilawa-Podgurski, A. Sagneri, and C. R. Sullivan, "Opportunities and challenges in very high frequency power conversion," in *Proc. Twenty-Fourth Annual IEEE Applied Power Electronics Conf. and Exposition (APEC)*, 2009.

[7] J. S. Glaser and J. M. Rivas, "A 500 W push-pull dc-dc power converter with a 30 MHz switching frequency," in *Proc. Twenty-Fifth Annual IEEE Applied Power Electronics Conf. and Exposition (APEC)*, 2010, pp. 654–661.

[8] N. Sokal and A. Sokal, "Class E-a new class of high-efficiency tuned single-ended switching power amplifiers," *IEEE Journal of Solid-State Circuits*, vol. 10, pp. 168–176, 1975.

[9] M. Iwadare, S. Mori, and K. Ikeda, "Even harmonic resonant class-E tuned power amplifier without RF choke," *Electronics and Communications in Japan (Part I: Communications)*, vol. 79, no. 1, pp. 23–30, 1996. [Online]. Available: http://dx.doi.org/10.1002/ecja.4410790103

[10] J. M. Rivas, Y. Han, O. Leitermann, A. D. Sagneri, and D. J. Perreault, "A high-frequency resonant inverter topology with low-voltage stress," *IEEE Transactions on Power Electronics*, vol. 23, no. 4, pp. 1759–1771, 2008.

[11] R. Erickson and D. Maksimovic, "A multiple-winding magnetics model having directly measurable parameters," in *Power Electronics Specialists Conference, 1998. PESC 98 Record. 29th Annual IEEE*, vol. 2, May 1998, pp. 1472–1478 vol.2.

[12] J. Glaser and J. Rivas, "A 500 W push-pull dc-dc power converter with a 30 MHz switching frequency," in *Applied Power Electronics Conference and Exposition (APEC), 2010 Twenty-Fifth Annual IEEE*, Feb 2010, pp. 654–661.